OPTOELECTRONICS AND ADVANCED MATERIALS – RAPID COMMUNICATIONS Vol. 12, No. 5-6, May-June 2018, p. 264 - 271

Projectile radiation calculation and spectrum detection rate of array CCD intersection measurement system

HANSHAN LI*, XIAOQIAN ZHANG, YANKE DING
School of Electronic and Information Engineering, Xi'an Technological University, Xi'an, 710021, China

To improve the testing accuracy and detection probability of the burst location parameter of projectile, this paper put forwards three infrared area array CCD intersection measurement method, sets up the infrared radiation characteristics model of projectile by using the surface element mesh analysis method and the bidirectional reflection distribution function, analyzes and derives the output signal function of projectile's radiation in unit area array CCD detection module; studies the relationship between the spectrum detection rate and the radiant energy, gives the calculation method and calculation function of detection rate of three infrared area array CCD. Through the calculation and analysis, the calculation results show the target radiant energy is maximum when the flight path of projectile is orthogonal with the optical axis of infrared area array CCD; the larger the radiation of projectile, the greater the spectrum detection rate of testing system; this paper gives the experiment result on the detection capture rate of three infrared area array CCD intersection measurement systems, the experimental results are basically consistent with theoretical calculations, which verify the calculation model is scientific.

(Received March 17, 2018; accepted June 7, 2018)

Keywords: Infrared area array CCD, Intersection measurement, Infrared radiation characteristics, Spectrum detection rate, Detection probability

1. Introduction

The imaging detection technology with high resolution and high sensitivity is currently an important research direction for the development of space target detection, especially with the development of photoelectron detection technology and testing device, the staring infrared focal plane detector is used in more and more research fields [1], such as the space debris detection, high-velocity target detection, the laser radar measurement and target tracking, which provides a more complete detection method for the industry development, national defense, agriculture and manufacturing industry.

Now the infrared photoelectric detection system is usually achieved in deep space for observation background, because the detection distance is far away or the detection temperature is very low, the photoelectric detection sensor gain the signal of target infrared radiation is very weak [2]. In the infrared photoelectric detection system, the thermal background radiation noise caused by the infrared receiving system's thermal radiation is one of the key factors to limit its detection sensitivity, at the same time, in low temperature, the infrared radiation energy and the difference of environmental radiation are not obvious, which greatly reduces the sensitivity of infrared photoelectric detection system [3]. In order to maximize the sensitivity of the infrared detection device, the whole cryogenic optical system is generally used, which has important significance to reduce radiation instrument noise, improve the detection sensitivity of testing system.

In weapon testing range field, the damage performance of projectile relies on the burst location parameters of projectile's fuze, while the burst location of projectile's fuze is closely related to the intersection echo characteristics between fuze and damage's target [4]. Since the intersection angle between the flight projectile's fuze and the damage's target is random, the space burst location of projectile fuze also is a random distribution. Usually, the burst location of projectile is the position that fuze was fired; it was called the projectile's burst location.

The acquisition of the burst location of projectile usually uses the visible-light photoelectric method, which is subject to the changes of the external environment temperature and illumination, meanwhile, this kind method is unable to obtain the target information under low illumination, so that the visible-light photoelectric method restricts the all-weather testing demand[5]. In order to realize the testing of burst location of projectile with high testing accuracy and high detection probability in all-weather, we use the infrared imaging technology to enhance the acquisition ability of projectile under the conditions of low temperature and low illumination.

According to the principle of three infrared area array CCD intersection measurement method, this paper researches and establishes the infrared radiation model and method of projectile and give scientific description the detection rate of infrared area array CCD intersection measurement system.

2. The testing principle of burst position parameters of projectile based on three infrared area array CCD

According to the intersection confrontation mechanism between damage's target and projectile's burst space location, the projectile's burst location mainly refers to the space position of projectile's burst instant during the projectile near to the damage's target in space, because the flight paths between projectile and damage's target forms a variety of intersection states, it produces the formation of multi-pose intersecting projectile's burst, the burst of projectile is interrelated with the damage's target under the multi-pose. In view of the characteristics of projectile and the testing requirement, we use the three infrared area array CCD intersection measurement method to set up the testing model of projectile's burst space location, Fig. 1 is its space geometry relation, we assume the height of damage's target is *H* from the ground, and the distance between the damage's target and the artillery is *L*, the coordination calculation is available based on reference[6] by any two area array CCD intersection measurement method. The first camera, second camera and third camera all are designed by using infrared area array CCD.

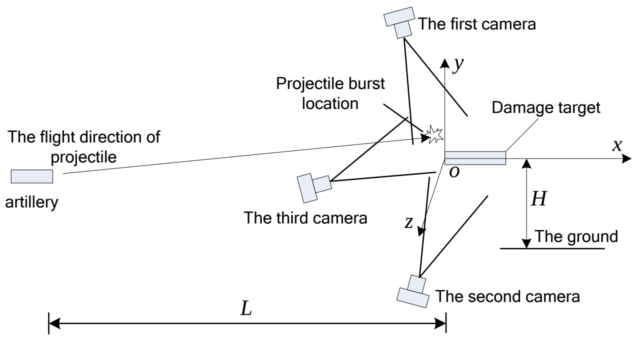

Fig 1. The model and relation on three infrared array CCD intersection measurements

In Fig. 1, the head of the damage target is original point of coordinate system, the placement requirements of three infrared array CCD are that the first camera and the second camera have a certain distance, and their optical axes are orthogonal layout, the optical axes orthogonal point is located the head of the damage target; From the direction of the artillery's launch, the third camera is located on between the gun and the across plane of the first camera and the second camera, and the distance between three infrared array camera is equilateral triangle. It is the basic requirements on the three infrared array CCD intersection placements.

From Fig. 1, it appears that to comprehensively access to burst location information of projectile, it is necessary to capture projectile's imaging information in the effective field of view based on three infrared area array CCD intersection measurement method, and the projectile's burst imaging information originate from projectile radiation energy. At different temperatures, the contributions of projectile radiation energy are different to infrared area array CCD, therefore, under different circumstance conditions, the detection ability of infrared area array CCD is playing an important role. To improve the capture rate of projectile's burst location, it is necessary to research the contribution of projectile's radiation and the detection rate of infrared area array CCD in three infrared area array CCD intersection measurement systems.

3. Radiation characteristics calculation model of projectile

In three infrared area array CCD intersection measurement systems, the imaging module of infrared area array CCD mainly include the optical lens, infrared photoelectric detector(namely, infrared area array CCD), detection processing module and image conversion module; the optical lens main gathers space projectile's imaging information, and then through the infrared area array CCD gain space projectile radiation energy, in accordance with detection processing module and image conversion module to gain the transient information of space projectile burst location. Because of the space projectile various gestures and forms, the contribution of space projectile radiation energy to the infrared photoelectric imaging system will become very different, in the complex environment, the environment illumination and temperature also greatly reduce the detection sensitivity of the infrared area array CCD, especially in low temperature environment, infrared characteristics of projectile appears to be inadequate. In order to improve detection sensitivity of the infrared photoelectric detector in the low temperature environment, we need to master the radiation characteristics of space projectile.

The space projectile is viewed as a cylinder, whose length is *l* and diameter is *D*. According to the state of projectile entering the optical field of infrared photoelectric imaging system, we use the surface element mesh analysis method to divide projectile surface into small unit grid of two dimensions, *n* and *m* are the number of two dimensions in evolving plane of projectile. By calculating the radiation characteristics of each small unit and using the superposition principle to calculate the whole radiation energy of projectile.

We use $\Delta S_{(i,j)}$ to express the (i, j) th unit surface of projectile, $\Delta S'_{(i,j)}$ is the imaging area of $\Delta S_{(i,j)}$ on the infrared array CCD detector, $\theta_{(i,j)}$ is the angle between the normal and the reflection of $\Delta S_{(i,j)}$, and H is the distance between the projectile and the optical objective, the optical imaging schematic diagram of projectile's unit area ($\Delta S_{(i,j)}$) is shown in Fig. 2.

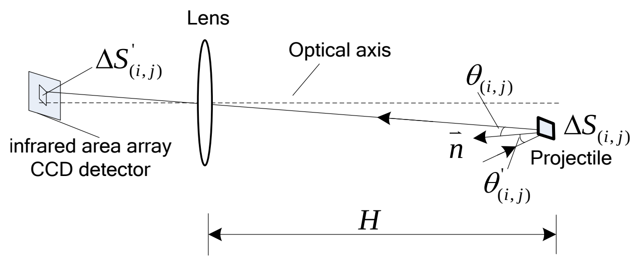

Fig. 2. The optical imaging schematic diagram of projectile's unit area

According to the space projectile unit area imaging detection principle, the optical characteristics of space projectile can be equivalent to the superposition of the surface element optical properties of the projectile discrimination. Fig. 3 shows the schematic diagram of projectile bidirectional reflectance in the photosensitive surface of infrared area array CCD detector, according to space projectile element imaging principle, the projectile's surface is decomposed into a series of independent panel set, we can calculate the reflection characteristics of each surface element to obtain the integral optical radiation characteristic function of space projectile.

Assuming $F_{(i,j)}$ is the discrete surface element's characteristic quantity, the characteristic parameters of the space projectile can be expressed as the set of $F_{(i,j)}$ in the unit of (i,j), the characteristic quantity of (i,j) th surface element is:

$$F_{(i,j)} = (p_{(i,j)}, \vec{n}, \Delta S_{(i,j)}, \varepsilon_{(i,j)}, \varpi_{(i,j)}, \psi_{(i,j)}) \tag{1}$$

In (1), $p_{(i,j)}$ is the center coordinate of surface element of projectile, which is $(x_{(i,j)}, y_{(i,j)}, z_{(i,j)})$, $\vec{n}$ is the normal direction of surface element, $\varepsilon_{(i,j)}$ is the diffuse reflectance of surface element, $\varpi_{(i,j)}$ is the illumination weighted factor of surface element, $\psi_{(i,j)}$ is the observation weighted factor of surface element [7-8].

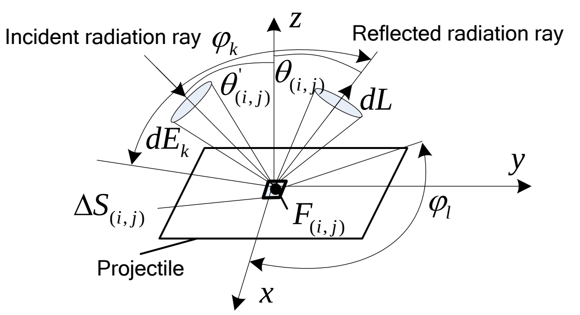

Fig. 3. The schematic diagram of projectile bidirectional reflectance in the photosensitive surface of infrared area array CCD detector

Reflection spectrum irradiance of projectile can be written as formula (2).

$$E(\lambda) = \sum_{i=1, j=1}^{n,m} E_{(i,j)}(\lambda) \cdot \varepsilon_{(i,j)} \cdot \psi_{(i,j)} \tag{2}$$

In (2), $E(\lambda)$ is the reflection spectrum irradiance of space projectile, $E_{(i,j)}(\lambda)$ is the reflection spectrum illumination of surface element, n and m are the number of surface element in two dimensional direction of projectile's total surface, the projectile's bidirectional reflection distribution function can be expressed by formula (3).

$$f_l(\theta'_{(i,j)}, \varphi_k, \theta_{(i,j)}, \varphi_l, \lambda) = \frac{dL(\theta'_{(i,j)}, \varphi_k, \theta_{(i,j)}, \varphi_l, \lambda)}{dE_k(\theta'_{(i,j)}, \varphi_k, \lambda)} \tag{3}$$

In (3), $\theta'_{(i,j)}$ and φ_k is the incident zenith angle and the incident azimuth angle, $\theta_{(i,j)}$ and φ_l is the reflected zenith angle and the reflected azimuth angle; λ is the spectrum radiation wavelength[9], dE_k is the incident radiation illuminance, dL is the reflection spectrum radiance.

$$L(\theta'_{(i,j)}, \varphi_k, \theta_{(i,j)}, \varphi_l, \lambda) = f_g(\theta'_{(i,j)}, \varphi_k, \theta_{(i,j)}, \varphi_l, \lambda) \cdot E_k(\theta'_{(i,j)}, \varphi_k, \lambda) \tag{4}$$

According to the photoelectric imaging principle of infrared area array CCD and the radiation characteristics of projectile, the radiant flux of the reflected background radiation on the surface of the (i, j) th unit at the entrance pupil of the infrared area array CCD detector can be expressed by formula (5).

$$\begin{aligned}\Phi_{(i,j)}(\lambda) &= \frac{1}{H^2} \Delta S_{(i,j)} \cdot S_r \cdot \cos\theta_{(i,j)} \cdot \cos^2\alpha \\ &\cdot \int_{\lambda_1}^{\lambda_2} f_l(\theta'_{(i,j)}, \varphi_k, \theta_{(i,j)}, \varphi_l, \lambda) \cdot E_k(\theta'_{(i,j)}, \varphi_k, \lambda) d\lambda\end{aligned} \tag{5}$$

In (5), α is the angle between the (i, j) th of projectile surface and the connection of the entrance pupil center to the optical axis, S_r is the area of the pupil in the detection optical system [10], then we can calculate the radiance of the reflected background radiation of the (i, j) th unit of projectile surface at the entrance pupil of the infrared area array CCD detector by formula (6).

$$\begin{aligned}E_{(i,j)}(\lambda) &= \frac{1}{H^2} \Delta S_{(i,j)} \cdot \cos\theta_{(i,j)} \cdot \cos^2\alpha \\ &\cdot \int_{\lambda_1}^{\lambda_2} f_l(\theta'_{(i,j)}, \varphi_k, \theta_{(i,j)}, \varphi_l, \lambda) \cdot E_k(\theta'_{(i,j)}, \varphi_k, \lambda) d\lambda\end{aligned} \tag{6}$$

Based on the theory of infrared area array CCD photoelectric imaging and the calculation principle of pupil energy, the radiation flux of the (i, j) th unit reflector background radiation on the infrared area array CCD detector is obtained by formula (7).

$$\begin{aligned}\Phi'_{(i,j)} &= \tau(\lambda) \cdot \frac{1}{H^2} \cdot \Delta S_{(i,j)} \cdot S_r \cdot \cos\theta_{(i,j)} \cdot \cos^2\alpha \cdot \\ &\int_{\lambda_1}^{\lambda_2} f_l(\theta'_{(i,j)}, \varphi_k, \theta_{(i,j)}, \varphi_l, \lambda) \cdot E_k(\theta'_{(i,j)}, \varphi_k, \lambda) d\lambda\end{aligned} \tag{7}$$

In (7), $\tau(\lambda)$ is the spectrum transmittance of optical system[10].

The irradiance of the (*i*, *j*) th unit reflecting background radiation in the projectile surface on the infrared area array CCD photosensitive surface is calculated as formula (8).

$$E'_{(i,j)} = \frac{1}{f(a+1)^2}\Delta S'_{(i,j)} \cdot \cos^4\alpha \cdot \int_{\lambda_1}^{\lambda_2} \tau(\lambda)\cdot f_l(\theta'_{(i,j)},\varphi_k,\theta_{(i,j)},\varphi_l,\lambda)\cdot E_k(\theta'_{(i,j)},\varphi_k,\lambda)d\lambda \tag{8}$$

In (8), a is the magnification of optical system.

Assuming that the target surface is composed of $n\times m$ units, the integral surface radiation of the target contributes to the radiant illumination of the infrared area array CCD detector is

$$E_t = \sum_{i=1,j=1}^{n,m} \frac{1}{f(a+1)^2}\Delta S_{(i,j)} \cdot \cos^4\alpha \cdot \int_{\lambda_1}^{\lambda_2} \tau(\lambda)\cdot f_l(\theta'_{(i,j)},\varphi_k,\theta_{(i,j)},\varphi_l,\lambda)\cdot E_k(\theta'_{(i,j)},\varphi_k,\lambda)d\lambda \tag{9}$$

Based on the radiation characteristics calculation model of projectile and the testing principle of three infrared area array CCD, the detection capability of each infrared area array CCD decide the capture rate of whole testing system, if we want to improve detection capability at long distance, it is necessary to increase the projectile's radiation are in infrared photosensitive CCD. Under the conditions of the field of view of optics lens, we should choose a telephoto lens with a large aperture to design its image unit system and improve imaging resolution.

4. The output function of infrared area array CCD

According to the projectile's infrared radiation characteristic calculation method and model, combined with the principle of infrared area array CCD photoelectric detection imaging, assuming that the projectile enters the optical field of infrared array CCD at any angle, the calculation model of formula (9) will turn to formula (10).

$$E = \cos\varphi \cdot E_t \tag{10}$$

In (10), φ is the optical axis angle between projectile and optical system of infrared area array CCD camera. The integral radiation output of the infrared area array CCD can be obtained by formula (11).

$$V_F = \tau_0\tau_1\int_{\lambda_1}^{\lambda_2}\left[(E-E_B)/H^2 - E_B\cdot\omega\right]\cdot S_r\cdot D^*(\lambda)d\lambda \tag{11}$$

In (11), E_B is the background radiance, ω is the optical field angle of the projectile relative infrared area array CCD, $D^*(\lambda)$ is the spectrum detection rate of infrared area array CCD. Here, $\omega = \sum_{i=1,j=1}^{n,m}\Delta S_{(i,j)}/H^2$ [11].

In order to obtain the total radiation of projectile in the infrared area array CCD, it is necessary to calculate its spectrum detection rate.

5. The calculation model and method of spectrum detection rate for infrared area array CCD

From the infrared radiation characteristics model of projectile, in order to improve projectile detection ability and gain high precision projectile's burst location parameters, we need to master the contribution of the infrared radiation of projectile's burst on infrared area array CCD, which have close relationship with the noise characteristics of the device itself and the detection sensitivity, therefore, it is necessary to establish the model for spectrum detection rate and sensitivity of infrared area array CCD.

According to the projectile radiation energy, the spectrum detection rate of the infrared area array CCD can be expressed by formula (12).

$$D^*(\lambda) = \int_{\lambda_1}^{\lambda_2}\frac{\eta}{hc\sqrt{\frac{(P_s+P_b)}{A_s}+\frac{I_0}{q}\frac{1}{A_s}+\frac{kT}{q^2}\frac{1}{RA_s}}}d\lambda \tag{12}$$

In (12), A_s is the photosensitive area of the infrared area array CCD detector, I_0 is the dark current, η is the quantum efficiency, k is the Boltzmann constant, R is the equivalent resistance of the infrared area array CCD detector, T is the absolute temperature, P_s is the signal power, and P_b is the background power. When $\frac{I_0}{q}\frac{1}{A_s}$, $\frac{kT}{q^2}\frac{1}{RA_s} \le \eta\frac{(P_s+P_b)}{A_s}$, the internal noise of the infrared area array CCD detector is mainly determined by the photon particle noise and the background noise [12], $D^*(\lambda)$ can be simplified as

$$D^*(\lambda) = \frac{\lambda}{hc}\sqrt{\frac{\eta A_s}{2(P_s+P_b)}} \tag{13}$$

In (13), the spectrum detection rate of infrared area array CCD detector is related to signal power, background power and CCD photosensitive area.

According to the spectrum detection rate function of infrared area array CCD, D^* indicate its normalized [13], and it can be written as formula (14).

$$D^* = \frac{V_s/V_n}{E_0}\left(\frac{\Delta f}{A_s}\right)^{1/2} \quad (14)$$

In (14), V_s/V_n is the output *SNR* of the infrared area array CCD detector, Δf is the noise frequency bandwidth, E_0 is the illuminance formed by the black body of a certain temperature. According to the function of spectrum detection rate, and combined with the formula (11), it is concluded that under the condition of a certain spectrum detection rate, the total radiation from the projectile's burst location to photosensitive area of the infrared area array CCD detector is deduced by formula (15).

$$V_F = \tau_0\tau_1\int_{\lambda_1}^{\lambda_2}\left[(E-E_B)/H^2 - E_B\cdot\omega\right]\cdot S_r\cdot\frac{V_s}{E_0 A_s}d\lambda \quad (15)$$

6. The calculation method of total detection rate in three infrared area array CCD intersection measurement method

The three infrared area array CCD intersection measurement method consists of a plurality of high-velocity infrared photoelectric imaging cameras intersection to acquire projectile's burst location, in order to establish detection ability calculation model of three area array infrared CCD, it need to be considered that the detection ability of three infrared area array infrared CCD in a comprehensive way.

According to the spectrum detection rate calculation model of unit infrared area array infrared CCD, the total spectrum detection rate of testing system can be described by formula (16).

$$D_t = \prod_{i=1}^{3}\frac{V_{si}/V_{ni}}{E_0}\left(\frac{\Delta f}{A_s}\right)^{1/2} \quad (16)$$

In (16), V_{si}/V_{ni} is the output signal to noise ratio of the i th infrared area array CCD detector.

From the (16), it shows that the spectrum detection rate of three infrared area array CCD intersection projectile's burst location parameters testing system depended on the spectrum detection rate of each infrared area array CCD, in order to obtain the all directions of projectile's burst location parameters, we need to improve the detection capability of each infrared area array CCD.

According to the calculation model and method of spectrum detection rate for infrared area array CCD, the output *SNR* of the infrared area array CCD detector will affect the spectrum detection rate, and the main influencing factors are the noise output of the system and the actual radiant energy of the projectile, from the formula (16), we know that the ratio of the noise output of the system (V_{ni}) and the actual radiant energy of the projectile (V_{si}) decide the total spectrum detection rate of testing system under the same background illumination, so, if the detection processing circuit of the infrared area array CCD is determined, the background noise of the system is basically determined, under this condition, the *SNR* of the system can be improved by increasing the radiant energy of the projectile, the specific measures are to increase the aperture or focal length of the optics lens, and increase the image area of projectile on the sensitive surface of the infrared area array CCD.

7. Calculation and experimental analysis

7.1. Calculation analysis

According to the infrared radiation characteristics model of projectile, we use the projectile that the diameter of projectile is 105 *mm* to calculate its infrared radiation energy and detection rate, the length of projectile about is 380 *mm*, suppose, the projectile is cylinder, the surface area of projectile about is 380 *mm*×330 *mm*, if each small element area is 10 *mm*×10 *mm*, the target surface is composed of *38*×*33* units.

Based on above the theory, we calculate the infrared radiation of flight projectile when it enters the optical field of infrared area array CCD at different angles, Fig. 4 gives the relation between the radiation area and radiation illuminance under different flight angles.

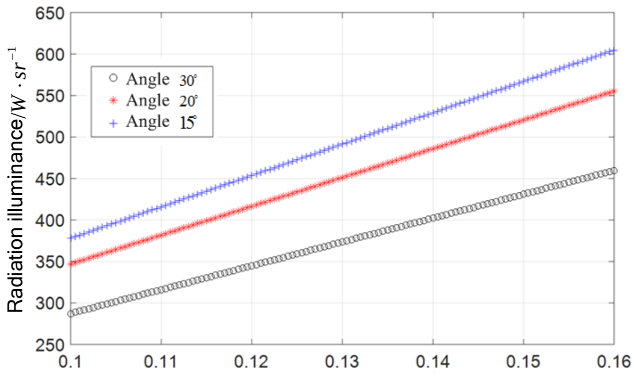

Fig. 4. The relation between the radiation area and radiation illuminance under different flight angles

In Fig. 4, it can be found that with the increase of the radiation area of flight projectile, the projectile radiation energy also increases; the radiation area of projectile is related to the viewing angle of infrared area array CCD, the smaller the angle between the optical axis and the flight projectile, the greater the radiation energy produced by projectile.

Based on formula (9), the detection distance is related to the infrared radiation characteristics of projectile, the transmittance of the optical system and the infrared band. Assuming that the transmittance of the optical system is 0.88, and the infrared band of CCD are a constant, so the radiation energy of projectile is inversely proportional to the square of detection distance. Fig. 5 gives the calculation results on the relationship between the detection distance and the radiation energy of projectile under the velocity of 730 m/s and 910 m/s respectively.

In Fig. 5, with the increments of detection distance, the radiation energy of projectile decreases gradually; under the same detection distance, the higher the projectile flight velocity, the higher the projectile's surface radiant energy, the main reason is that the higher the velocity of projectile, the higher the friction heat it generates from the air and projectile, it make the radiation energy of projectile increase.

According to the formula (14), under the condition that signal to noise ratios are $3dB$, $4dB$ and $5dB$ respectively. Fig. 6 gives the calculation results on the radiation energy and the spectrum detection rate of infrared area array CCD.

From Fig. 6, if the radiation energy of projectile increases, the spectrum detection rate of infrared area array CCD also increases. In order to describe the spectrum detection ability of the whole testing system, it need to synthetically consider the spectrum detection rate of three area array CCD detector, based on the formula (16), we give the calculation results on the relationship between spectrum detection rate and signal to noise ratio in three infrared area array CCD intersection measurement, as shown in Fig. 7.

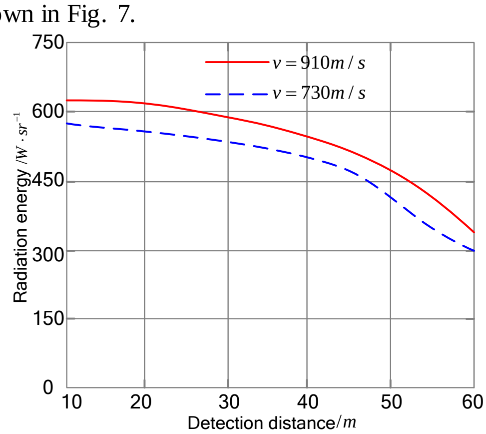

Fig. 5. The calculation results on the relationship between the detection distance and the radiation energy of projectile

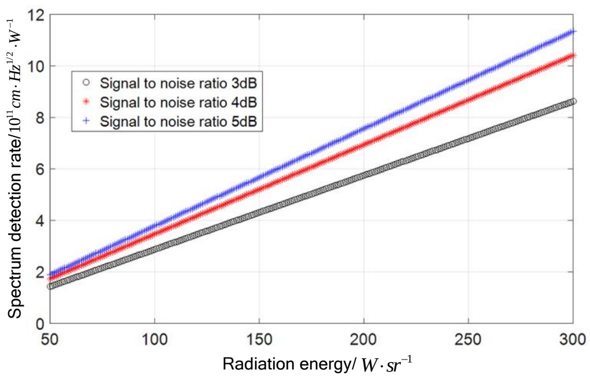

Fig. 6. The change curve between radiation energy and spectrum detection rate of infrared area array CCD

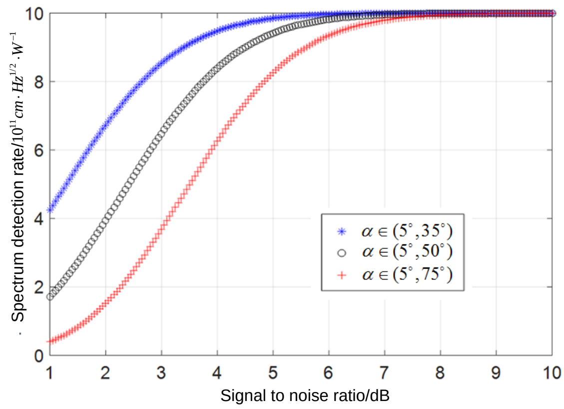

Fig. 7. The change curve between spectrum detection rate and signal to noise ratio

According to Fig. 7, with the increment of signal to noise ratio, the system spectrum detection rate increases gradually; by adjusting the effective viewing field between any two infrared area array CCD in testing system, so that the angle between flight projectile and optical field in unit infrared area array CCD are suitable, it can improve the detection rate, and then, the spectrum detection rate of three infrared area array CCD intersection measurement will be improved.

In order to effectively improve the system capture rate, we require a combination of three cameras detection rate to consider and analyze, in general, if the detection rate higher is, the capture rate will be increased; on the other hand, we can increase the optical aperture, it make the radiation energy of projectile increase, and the signal to noise ratio of the system also improve, the acquisition rate of the whole test system will make a great improvement.

7.2. Experiment and analysis

Based on projectile's radiation characteristics and the detection performance on infrared array CCD, we use the detection capture rate of three infrared area array CCD intersection measurement systems to verify the correctness of projectile's radiation characteristics and spectrum detection rate.

The establishment of the intersection test platform by three infrared area array CCD, we test the burst location of projectile that the diameter is 105 *mm*, the focal length of lens of infrared area array CCD is 125 mm, the experimental conditions is that the height of damage's target is 16.1 m and the distance between the first camera and the second camera is 14.5 m, the lay of first camera and second camera is orthotropic with projection of damage's target, the third camera is placed in front of the projection of damage's target according to Fig. 1. Under those experimental conditions, we test ten projectile's burst location relative to the damage's target in one experiment, the origin of coordinate the testing system set in the head of damage's target.

Table 1 and Table 2 are the testing results, Table 1 is the burst location of projectile, Table 2 is the corresponding average output voltage and the spectrum detection rate of infrared area array CCD, the inherent noise of system about is 3.5V, and the unit of spectrum detection rate is $10^{11} cm \cdot Hz^{1/2} \cdot W^{-1}$ in infrared area array CCD, we use spectrum detection rate to describe the detection probability.

Table 1. The burst location test data of Projectile

NO.	*X*(m)	*Y*(m)	*Z*(m)
1	2.32	-3.16	-1.38
2	-1.67	-3.03	-1.56
3	-1.22	-3.67	-1.23
4	-1.09	-4.34	1.26
5	-1.11	-4.73	-1.37
6	1.73	-3.91	2.11
7	-2.62	-3.55	-0.98
8	-1.18	-3.87	-1.52
9	1.65	-4.59	1.21
10	-2.43	-4.21	-1.32

Table 2. The corresponding average output voltage and the spectrum detection rate of infrared area array CCD

NO	first camera		second camera		third camera	
	average output voltage (V)	spectrum detection rate	average output voltage (V)	spectrum detection rate	average output voltage (V)	spectrum detection rate
1	5.22	6.56	5.38	6.85	5.83	6.87
2	6.28	7.21	6.13	7.68	6.65	8.16
3	4.19	5.81	6.52	7.96	6.87	8.38
4	6.09	7.18	6.84	8.15	7.21	8.62
5	6.26	7.29	-	-	7.57	8.84
6	5.93	6.98	7.12	8.43	7.14	8.53
7	6.76	8.02	6.98	8.53	6.96	8.41
8	6.33	7.34	7.01	8.01	7.15	8.69
9	6.09	7.19	6.17	7.79	7.39	8.67
10	5.68	6.86	5.66	6.67	7.02	8.49

According to the collected signals in Table 2, it can be found that in a certain signal to noise ratio and spectrum detection rate, we can calculate the burst location of projectile, when the signal to noise ratio is less than 3dB, the spectrum detection rate is significantly reduced, which shows that the projectile radiation energy may be smaller, the distance may exceed the burst condition of theory burst range of projectile. Combining with Table 1, we can come to conclusion that as the increase of the distance, the output signal decreases, the detection rate also is reduced, such as the NO.2 burst location of projectile is (-1.67, -3.03, -1.56), the output signal of the first camera is 6.28V, the output signal of the second camera is 6.13V, the output signal of the third camera is 6.65V; the NO.5 burst location of projectile is (-1.11, -4.73, -1.37), the output signal of the first camera is 6.26V, the output signal of the second camera is 6.16V, the output signal of the third camera is 7.57V. Comparing with burst locations of projectile from the Z axis between the NO.2 and NO.5, NO.5 burst location of projectile is closer to the second camera, in the same of the second camera, the output signal of NO.5 is greater than the NO.2; Comparing with burst locations of projectile from the Y axis between the NO.2 and NO.5, the detection distance of the NO.5 is smaller, in the same of the third camera, the output signal of NO.5 is greater than the NO.2. Based on Table 2 and formula (16), we calculate the total spectrum detection rate of the testing system about is $8.5 \times 10^{11} cm \cdot Hz^{1/2} \cdot W^{-1}$. The output information both come from the projectile's radiation, because of the different angle between each CCD and projectile's attitude, the radiation reception of the projectile by CCD sensor will be different.

Based on the above experimental data, it deduce that the detection rate of three area array CCD cameras are complementary to each other, in accordance with the testing principle of three infrared area array CCD intersection measurement method, the burst location parameters of projectile can be obtained by combining between every two cameras, and the use of three cameras to gain projectile's information, which increases the capture rate of the whole system.

This experiment also verifies the projectile's radiation characteristics calculation model and spectrum detection rate function is reasonable, within the limit detection range, we test multiple projectile's burst location, and find the infrared area array CCD the capture rate of three infrared area array CCD intersection measurement system can reach 98.3%, but, based on the method of literature [14] and [15], the capture rate about is 88.9%, it also reflect use three infrared area array CCD intersection measurement method that can improve the detection probability.

8. Conclusions

According to the testing platform of projectile's burst location by using three infrared area array CCD intersection measurement method, this paper studies the target infrared radiation characteristics of projectile and detection rate of testing system by using the surface element mesh analysis method and the bidirectional reflection distribution function, give out the projectile surface total radiation calculation model, and derives the output calculation function of single area array CCD sensor radiation signal, analyses the influence of the background illumination and the spectrum detection rate to the output signal and gives the total detection rate calculation function on three infrared area array CCD. Through the calculation and experiment, this paper gives the effects relation the projectile radiation illumination and different detection distance, and the relation between spectrum detection rate and target radiation energy, the calculation results show when the flight angle of projectile and the imaging axis of infrared area array CCD is orthogonal, the radiation energy of projectile is maximum under the same detection distance, the radiation output of the infrared area array CCD is inversely proportional to the distance; the testing method of projectile's burst location by using three infrared area array CCD intersection measurement model can improve the detection rate and capture rate, and the radiation characteristics calculation model of projectile and the calculation method of spectrum detection rate for infrared area array CCD are scientific and feasible.

Acknowledgment

This work has been supported by Project of the National Natural Science Foundation of China (No. 61773305) and the Key Programs of Shaanxi science and Technology Department (No.2017GY-037).

References

[1] An Ying, Ni Jinping, Journal of Xi'an Technology University **26**(3), 515 (2007).
[2] Dong Hua, Wang Tieling, Ni Jinping, Opto-electronic Engineering **36**(1), 17 (2009).
[3] Song Chunhuan, Gao Junchai, Zhang Xiaoqian, J. Optoelecton. Adv. M. **17**(1-2), 7 (2015).
[4] Tan Yayun, Zhang He, Cha Bingting, High Power Laser and Particle Beams **27**(11), 111012-1 (2015).
[5] Liu Wen, Xiong Rensheng, Zhang Yunqi, Acta Photonica Sinica **37**(2), 413 (2008).
[6] T. Bitao, C. Hongbin, W. Qunshu, G. Xiaowei, Acta Photonica Sinica **42**(11), 1340 (2013).
[7] W. Diao, X. Mao, X. Liang, Journal of Beijing University of Aeronautics and Astronautics **35**(8), 1022 (2009).
[8] Hanshan Li, Applied Optics **55**(13), 3689 (2016).
[9] H. Wu, X. Yi, International Journal of Infrared and Millimeter Waver **24**(12), 2059 (2003).
[10] Zhang Baohui, Zhang Junju, Chang Benkang, Acta Armamentarii **33**(11), 1319 (2012).
[11] Wand Shi-Tao, Zhanu Wei, Wand Qiang, Optics and Precision Engineering **20**(3), 487 (2012).
[12] Zhang Guoqing, Liu Lina, Zhu Changjun, Infrared and Laser Engineering **42**(7), 1819 (2013).
[13] X. Mao, L. Chang, W. Diao, Journal of Beijing University of Aeronautics and Astronautics **37**(11), 1429 (2011).
[14] Hanshan Li, Zhiyong Lei, Optics and Precision Engineering **20**(2), 329 (2012).
[15] Dong Tao, Ni Jinping, Optical Technique **37**(4), 406 (2011).

*Corresponding author: lihanshan269@163.com